Resolved donor-acceptor pair-recombination lines in diamond luminescence

B. Dischler, W. Rothemund, C. Wild, R. Locher, H. Biebl, and P. Koidl
Fraunhofer-Institut für Angewandte Festkörperphysik, Tullastrasse 72, D-79108 Freiburg, Germany
(Received 16 July 1993)

Cathodoluminescence has been investigated in diamond films, prepared by microwave plasma assisted chemical-vapor deposition. Results are presented for various diamond films differing in crystalline structure and doping. In the energy range 2.0–2.7 eV a series of 13 sharp luminescence lines has been observed at temperatures below 200 K. In a tentative interpretation they are attributed to donor-acceptor pair recombination. The Coulomb energy depends on the discrete values for the pair separation in the expected manner including a Bohr radius correction for the three closest pairs. The relative intensities of the lines depend on the growth conditions and on the film texture. Likely candidates for the pairs are the nitrogen donor and the boron acceptor. Both impurities are contained in the present samples. The sum of the binding energies is 3.57 eV, and inserting $E_a = 0.37$ eV for boron yields $E_d = 3.2$ eV for nitrogen.

INTRODUCTION

Luminescence from (high-pressure) synthetic and natural diamond[1,2] and more recently from (low-pressure) chemical-vapor-deposited (CVD) diamond[2,3] has been investigated and reported in detail. The luminescence, which is observable in almost all types of diamond, is a sensitive detection method for identified defects,[2] e.g., isolated vacancies (GR1 at 1.673 eV), the carbon ⟨100⟩ split interstitial (5RL at 4.582 eV), a silicon-related center (at 1.681 eV), several nitrogen-related centers (see below), and bound excitons (for boron at 5.21 eV). It is desirable to obtain an interpretation for those lines which are not yet assigned.

The preparation of diamond films using CVD techniques is now well established, and these films show a great variety of growth morphology and impurity content.[3] Considerable variations have been observed in the corresponding cathodoluminescence (CL) and photoluminescence (PL) spectra, which consist of broadbands and sharp lines.[2–6]

In the present work, data on additional sharp CVD diamond luminescence lines are presented, and an assignment in terms of resolved donor-acceptor pair recombination (DAPR) is given. The DAPR luminescence consists of a regular series of lines, because the Coulomb contribution to the energy of the emitted light depends on the donor-acceptor pair separation, for which only discrete values exist in the lattice. Sharp DAPR luminescence lines have been reported for other host crystals like silicon[7] or GaP.[8] The many interesting practical and theoretical aspects of DAPR, including electronic compensation or recombination of trapped carriers and several types of interaction, have been reviewed.[9] For the investigation of impurities in diamond it is important to obtain a positive confirmation of the present interpretation, i.e., resolved DAPR from a nitrogen donor and a boron acceptor. It would provide, to our knowledge, the first spectroscopic determination of the binding energy of the nitrogen donor, and it would be, to our knowledge, the first example of stable electron and hole trapping at the nearest-neighbor pair. The new results should also assist in an explanation for the broad "*A*" band luminescence in the energy range 2–4 eV, which has been attributed to unresolved DAPR.[1]

Part of the sharp lines, which are now assigned to DAPR in diamond, have probably been seen previously as weak signals by several authors.[10–14] However, the luminescence lines[10–13] have not been interpreted and only the lines at 2.67, 2.50, and 2.20 are contained in a recent listing.[2] The corresponding absorption lines have been observed in synthetic diamond, heat treated at 1700 °C; these lines have been assigned to intermediate stages of nitrogen aggregation.[14]

EXPERIMENT

The lines to be discussed below have been seen in more than 30 diamond films which were prepared by microwave plasma assisted CVD as described previously.[15,16] Three different samples have been selected, which in the following are named *A*, *B*, and *C*. Sample *A* is a boron-doped polycrystalline diamond film, grown on a silicon substrate at 820 °C and 50 mbar from 1.5% CH_4 in H_2. The film thickness is 21 μm and the boron-doping level is 20 ppm. The film contains nitrogen as is evident from a strong CL line at 575 nm from the 2.16-eV (nitrogen plus vacancy) center and lines at 441 and 389 nm from the nitrogen containing 2.81- and 3.19-eV centers.[2,17] Sample *B* is a nominally undoped homoepitaxial film, grown on a polished {100} natural diamond plate, which was placed on a *p*-type (boron-doped) silicon substrate. The film thickness is 155 μm and nitrogen is present leading to CL lines from the 2.16-, 2.81-, and 3.19-eV centers, similar to sample *A*. Also an intense ESR signal from the substitutional nitrogen donor is observed.[18] Sample *C* is a polycrystalline diamond film on a silicon substrate, and its preparation at a temperature of 980 °C is described in Ref. 16. The film thickness is 16 μm. Sample *C* is boron contaminated[12] and contains ni-

trogen, causing a weak CL from the 2.16-eV center. Much silicon is incorporated in this sample,[16] leading to a very intense CL line at 737 nm from the 1.68-eV (silicon plus vacancy) center.[2,4,19]

The CL was excited with a defocused electron beam at a voltage of 25–35 kV and a current of 0.5–1.5 μA. The penetration depth of the electron beam is ~ 5 μm. The sample temperature was 77 K (for other temperatures see below). The CL emission was collected with a paraboloid mirror, dispersed in a 0.5-m monochromator and detected with a photomultiplier. No corrections were made for wavelength-dependent sensitivity of the instrument. Infrared spectroscopy was used to evaluate (i) the thickness and (ii) the boron acceptor concentration of CVD diamond films, using (i) the interference fringes and (ii) the boron-related absorption at 2802 and 3050 cm^{-1}.[2] The boron absorption is weak in thin films with low boron content; therefore parallel samples with > 100 ppm boron were used for calibration.

RESULTS AND DISCUSSION

The CL spectra of the CVD diamond samples *A*, *B*, and *C* are shown in Fig. 1. The spectrum of sample *C* in Fig. 1(c) shows a characteristic series of lines. Samples *A* and *B* exhibit the same lines as sample *C*, however with different relative intensities. Based on the similarity to the DAPR luminescence spectra in silicon[7] and GaP (Ref. 8) we tentatively assign the spectra in Fig. 1 to DAPR luminescence in diamond. The shell numbers, which are used to label the discrete donor-acceptor pair separations,[9,20] are indicated in Fig. 1(c). Beyond the sixteenth shell the DAPR lines are weak and not well resolved. The slightly broader line at 551 nm [see Figs. 1(a) and 1(b)] arises from the nitrogen-related 2.25-eV center[2] and does not belong to the DAPR series.

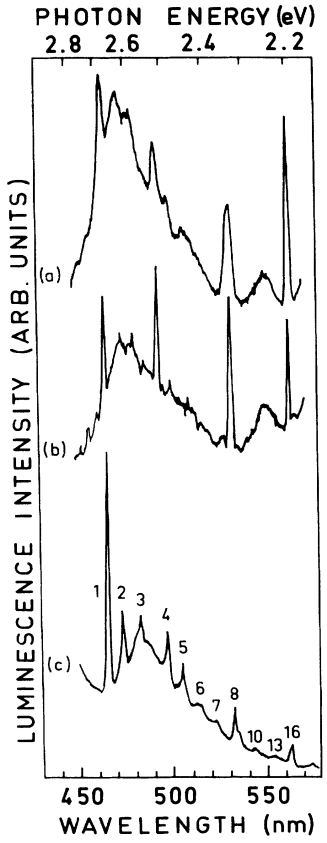

FIG. 1. Cathodoluminescence spectra of three different CVD diamond samples, taken at 77 K. Spectrum (a) is from the boron-doped polycrystalline sample *A*, spectrum (b) is from the nominally undoped {100} epitaxial sample *B*, and spectrum (c) is from the boron-contaminated polycrystalline sample *C*. Shell numbers (see Table I) are indicated in spectrum (c).

Preliminary results on the temperature dependence of the CL were obtained by taking additional spectra at 20, 150, 200, and 300 K. The linewidths, which are between 6 and 23 meV at 77 K, decrease slightly at 20 K and increase slightly at 150 K. Above 200 K the DAPR series is no longer observable with CL, however a line at 2.32 eV (534 nm) persists at least up to 300 K. This line is evidently from a different origin[6] but almost coincides with the DAPR line from the eighth shell at 2.33 eV (532 nm), and can be seen as a shoulder in Fig. 1(c).

According to Refs. 1, 7, and 8 the energy of the DAPR lines is given by Eq. (1),

$$h\nu = E_g - E_a - E_d + (e^2/\epsilon r) - E_{\text{corr}} \ . \tag{1}$$

Here E_g is the band-gap energy, E_a and E_d are the binding energies of the acceptor and donor, e is the electronic charge, ϵ is the static dielectric constant, r is the distance between acceptor and donor, and E_{corr} is a correction term, which vanishes for large pair separations.[1,7,8] The fourth term, arising from the Coulomb interaction between the ionized donor and acceptor, is of special interest. With acceptor and donor on substitutional lattice sites, the pair separation r can assume only discrete values, which can be obtained by inserting the shell number m into Eq. (2),

$$r_b/r = [0.75/(m-x)]^{1/2} \ . \tag{2}$$

Here r_b is the C-C bond length (0.1545 nm), and $x = 0.25$ for odd-shell numbers while $x = 0$ for even-shell numbers m.[20]

It follows from Eq. (1) that for vanishing E_{corr} a plot of the photon energies versus the inverse pair separation $1/r$ should result in a straight line with a slope of e^2/ϵ. Using the normalized pair separation r_b/r as the abscissa yields a slope of $e^2/\epsilon r_b$, and this is shown in Fig. 2.

In Table I data on the DAPR series are collected. Columns 2, 3, and 4 are given for the diamond lattice, where the statistical abundance (in column 4) is the number of equivalent pairs in the respective shell.[9,20] The observed energies (in column 5) are slightly sample dependent, e.g., between 2.66 and 2.68 eV for line number 1. By fitting the observed luminescence energies of the shell numbers 4–16 to Eq. (1), the numbers in Eq. (3) are obtained,

$$h\nu \ (\text{eV}) = 1.89 + 1.44 r_b/r \ . \tag{3}$$

The observed energies in column 5 of Table I agree within 0.01 eV with the values resulting from Eq. (3), ex-

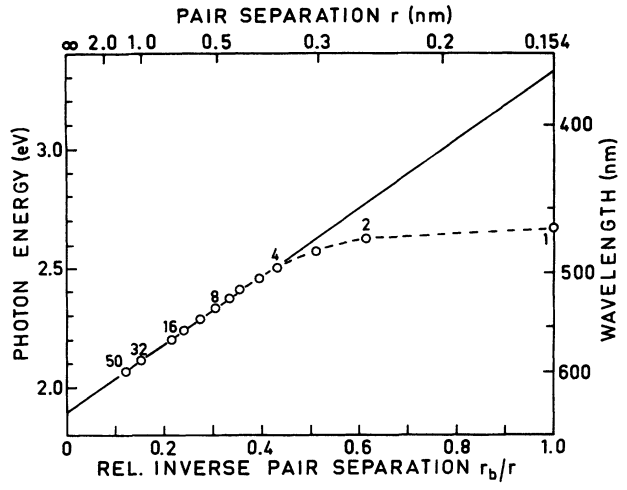

FIG. 2. Plot of the observed luminescence line energy as a function of the relative inverse pair separation. Relevant shell numbers are indicated. The straight line gives the calculated Coulomb energy for point charges. The broken line connects the experimental points. The top scale gives the separation of the donor-acceptor pairs. The right scale gives the wavelength of the luminescence lines.

cept for the shell numbers 1–3 (see below). This is strong support for the present interpretation.

The slope in Fig. 2 is 1.44 eV [see Eq. (3)]. This value is close to 1.64 eV, as predicted for diamond.[1] Note that this slope is identical with the maximum possible Coulomb energy, and that the theoretical expression $(e^2/\varepsilon r_b)$ contains crystal-specific constants but does not depend on the nature of the donor and acceptor. The slight difference between the predicted[1] and observed slope may disappear when inserting the dielectric constant for the present CVD diamond films, and also allowing for possible perturbations from the pair forming defects. The Coulomb energies for the shells 1–3 fall below the straight line in Fig. 2, and this is expected because in Eq. (1) without the correction term E_{corr} point charges are assumed, while the true charges of donor and acceptor extend out to the Bohr radius. Similar deviations have been found in the DAPR series in silicon[7] and GaP (Ref. 8) for pair separations smaller than the Bohr radius.

The last column of Table I gives a listing of the energies, which have been previously observed in absorption.[14] The differences to the luminescence energies in column 5 are between 0 and 0.03 eV. Remarkable is the splitting of 0.01 eV observed in absorption[14] between lines 7*a* and 7*b*. This splitting confirms the present as-

TABLE I. Calculated data for the DA pairs in diamond and observed line positions for DAPR in luminescence and absorption.

Shell No.	r (nm)	Lattice vector	Statist. abund.	$h\nu^a$ (luminesc.) (eV)	$h\nu^b$ (absorpt.) (eV)
1	0.154	⟨1,1,1⟩	4	2.67	2.65
2	0.252	⟨2,2,0⟩	12	2.62	2.62
3	0.296	⟨3,1,1⟩	12	2.57	2.57
4	0.357	⟨4,0,0⟩	6	2.50	2.48
5	0.389	⟨3,3,1⟩	12	2.46	2.43
6	0.437	⟨4,2,2⟩	24	2.41	2.41
7*a*	0.463	⟨3,3,3⟩	4	2.37	2.38
7*b*	0.463	⟨5,1,1⟩	12	2.37	2.39
8	0.504	⟨4,4,0⟩	12	2.33	2.35
9	0.528	⟨5,3,1⟩	24		
10	0.564	⟨6,2,0⟩	24	2.28	2.29
11	0.585	⟨5,3,3⟩	12		
12	0.618	⟨4,4,4⟩	8		
13*a*	0.637	⟨7,1,1⟩	12	2.24	2.24
13*b*	0.637	⟨5,5,1⟩	12	2.24	2.24
14	0.667	⟨6,4,2⟩	48		
15*a*	0.685	⟨7,3,1⟩	24		
15*b*	0.685	⟨5,5,3⟩	12		
16	0.713	⟨8,0,0⟩	6	2.20	
32	1.009	⟨8,8,0⟩	12	2.11	
50*a*	1.261	⟨10,10,0⟩	12	2.07	
50*b*	1.261	⟨14,2,0⟩	24	2.07	
50*c*	1.261	⟨10,8,6⟩	48	2.07	

[a]Present work.
[b]From Ref. 14, Table I and Fig. 1(c).

signment; it is caused by a weak multipole interaction.[9]

The integrated intensities of the observed lines are shown in Fig. 3. Normalized values on a logarithmic scale are plotted versus the shell number. The normalization is performed by taking the sum of the intensities of lines 1–16 as 100%, both for the observed and for the theoretical intensities. Then the observed intensities are divided by the respective theoretical values. If the observed intensities would match the statistical abundance of the respective shell, all normalized values would be 1, as indicated by the dashed horizontal line in Fig. 3. However, the experimental results in Fig. 3 show that the intensities of the shells No. 4, 8, and 16 appear as spikes with values an order of magnitude higher than expected from the statistical abundance.

The intensity spikes in Fig. 3 for the pairs with lattice vectors ⟨4,0,0⟩, ⟨4,4,0⟩, and ⟨8,0,0⟩ (shells 4, 8, and 16) are not understood at present. The spikes are especially pronounced for the {100} homoepitaxial sample *B*, which has {100} growth sectors only. In sample *C* [Fig. 1(c)] a variety of growth sectors occurs and up to shell 16 almost all shells are occupied, but again the pairs in shells No. 2, 4, 8, and 16 have higher intensities (see Fig. 3). Among the weaker lines beyond shell No. 16 (see Table I), the pairs in shell No. 32 ⟨8,8,0⟩ and No. 50*a* ⟨10,10,0⟩ have the same orientation as in shell No. 8 ⟨4,4,0⟩. The expected higher intensity would explain why among the weak lines only these shells are observed. The intensities of the DAPR lines observed in absorption in a high-pressure synthetic diamond[14] indicate similarities, e.g., the lines from shells No. 9, 11, and 12 are below the detection limit, both in absorption and in luminescence. This is in contrast to their relatively high statistical abundance. The absorption measurements are also remarkable with respect to Coulomb attraction and diffusion, because after heating to 1700 °C no pairs with shell numbers higher than 13 were observed, and after heating to 2400 °C only the lines at 2.65 and 2.62 (shells No. 1 and 2) had remained.[14]

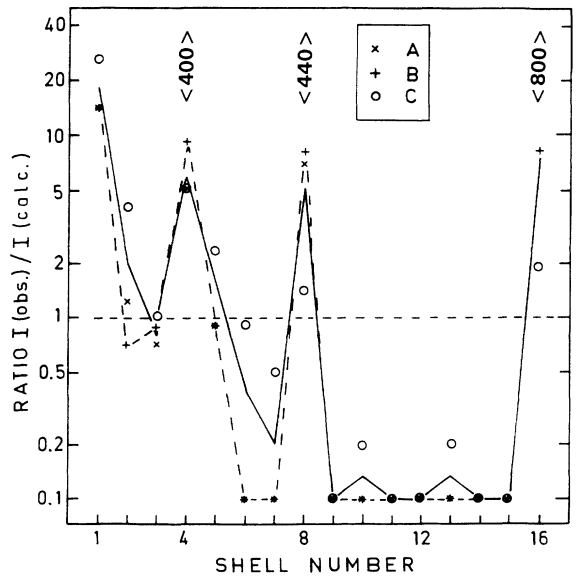

FIG. 3. Ratio of the observed-to-calculated line intensities as a function of the shell number for the three samples *A* (×), *B* (+), and *C* (○). The full curve is the average for the three samples, the long-dashed curve is for the epitaxial sample *B*, and the short-dashed line (with constant value 1) corresponds to the theoretical statistical abundance. Relevant pair orientations are indicated.

Inserting $E_g = 5.48$ eV into Eqs. (1) and (3) yields the sum of the binding energies:

$$E_d + E_a = E_g - 1.89 = 3.57 \text{ eV} . \quad (4)$$

A well-known acceptor in diamond is substitutional boron with a binding energy of 0.37 eV.[2] The assumption of boron as the acceptor is supported by the observation in additional samples where the reduction of the boron doping level from 20 to 2 ppm reduced the DAPR intensity by approximately the same proportion. Inserting $E_a = 0.37$ into Eq. (4) yields $E_d = 3.20$ eV. A deep donor in diamond is isolated nitrogen and a binding energy of 3.2 eV is in the expected range. The experimental estimates for $E_d(N)$ are between 1.7 and 4.1 eV,[2,21] and the theoretical values are 3.3 and 4.3 eV.[21] Thus, both from the known impurity content of the samples and from the derived binding energies it can be concluded that nitrogen and boron are the most likely candidates for the observed *D-A* pairs.

A comparison can be made with the DAPR series in Si:P,In (Ref. 7) and GaP:S,Zn,[8] where the donors and acceptors have low binding energies (45–155 meV) and the close pairs [shells with numbers below 5 (Si) or 14 (GaP)] are not observed in luminescence. This has been explained by the insufficient stability of the "excited" close pairs and it has been predicted[8] that in materials with larger binding energies the close pairs should be observable in DAPR. This is now found for diamond with the close pairs down to the first shell.

The total intensity of the DAPR is temperature independent in the range 20–100 K. It is reduced to 50% at 150 K and approaches zero near 200 K. Using the simple empirical model of Ref. 6 yields a thermal activation energy of the order 0.2 eV, which is comparable to the acceptor binding energy of 0.37 eV. The relative intensities of close and distant DA pairs are independent of temperature. Changing the exciting beam current by a factor of 3 changed the total intensity proportionally, while the relative line intensities remained unchanged.

More work is necessary to establish the conditions under which the resolved DAPR lines can be observed. The lines have been observed in CVD diamond (present work and Refs. 11–13), in high-pressure synthetic diamond,[14] and in natural diamond.[10] The presence of nitrogen and boron is positively known for most of the samples which show the DAPR lines. The DAPR lines are sharper in epitaxial CVD samples, but are also observed in polycrystalline samples for which the Raman spectrum indicates low crystalline quality. It must be emphasized that very close to the positions of lines 3 and 8 [see shoulders in Fig. 1(c)] and probably also close to the positions of lines 4 and 5 (see Ref. 13) other lines can appear, which do not belong to the DAPR series.

CONCLUSIONS

In summary, a series of sharp CL lines has been observed in polycrystalline diamond films, prepared by microwave plasma assisted CVD. In a tentative interpretation the lines are assigned to DAPR with specific pair separations. A plot of the CL photon energies versus inverse pair separation yields a slope of 1.44 eV, which is close to the predicted theoretical value of 1.64 eV. The present samples contain nitrogen and boron, which are likely candidates for the pair forming donor [$E_d(N)=3.2$ eV] and acceptor [$E_a(B)=0.37$ eV].

The first identification of resolved DAPR lines in diamond is of both experimental and theoretical interest. Future systematic studies should reveal whether the relationship between growth morphology and the intensity of particular lines can be exploited. Since the formation of the very close DA pairs involves diffusion, more insight into relationships between the deposition parameters and the diffusion of impurities may be obtained by monitoring the relative abundance of the closest pairs. A better understanding of the types of incorporation of electronically and optically active defects is also of vital interest for future applications of diamond.

ACKNOWLEDGMENTS

Valuable discussions with N. Herres, J. Schneider, and J. Wagner are acknowledged. The authors thank T. Eckermann and K. Schmidt for expert technical assistance. We acknowledge A. Badzian, Pennsylvania State University, for kindly providing sample *C*.

[1]P. J. Dean, Phys. Rev. **139**, A588 (1965).

[2]*The Properties of Natural and Synthetic Diamond,* edited by J. E. Field (Academic, London, 1992); especially Chap. 2 by C. D. Clark, A. T. Collins, and G. S. Woods.

[3]See Diamond Relat. Mater. **2**, 59 (1993).

[4]V. S. Vavilov, A. A. Gippius, A. M. Zaitsev, B. V. Deryagin, B. V. Spitsyn, and A. E. Aleksenko, Fiz. Tekh. Poluprovodn. **14**, 1811 (1980) [Sov. Phys. Semicond. **14**, 1078 (1980)].

[5]A. T. Collins, M. Kamo, and Y. Sato, J. Phys. D **22**, 1402 (1989).

[6]Y. L. Khong and A. T. Collins, Diamond Relat. Mater. **2**, 1 (1993).

[7]W. Schmid, U. Nieper, and J. Weber, Solid State Commum. **45**, 1007 (1983).

[8]D. G. Thomas, M. Gershenzon, and F. A. Trumbore, Phys. Rev. **133**, A269 (1964).

[9]P. J. Dean, in *Progress in Solid State Chemistry,* edited by J. O. McCaldin and G. Somorjai (Pergamon, Oxford, 1973), Vol. 8, p. 1.

[10]P. J. Dean and J. C. Male, J. Phys. Chem. Solids **25**, 1369 (1964).

[11]A. T. Collins, M. Kamo, and Y. Sato, in *Diamond, Silicon Carbide and Related Wide Bandgap Semiconductors,* edited by J. T. Glass, R. Messier, and N. Fujimori, MRS Symposia Proceedings No. 162 (Materials Research Society, Pittsburgh, 1990), p. 225.

[12]B. G. Yacobi, A. R. Badzian, and T. Badzian, J. Appl. Phys. **69**, 1643 (1991).

[13]J. Ruan, K. Kobashi, and W. J. Choyke, Appl. Phys. Lett. **60**, 3138 (1992).

[14]A. T. Collins and M. Stanley, J. Phys. D **18**, 2537 (1985).

[15]C. Wild, W. Müller-Sebert, T. Eckermann, and P. Koidl, *Materials Science Monographs* (Elsevier, Amsterdam, 1991), Vol. 73, p. 197.

[16]A. R. Badzian, T. Badzian, R. Roy, R. Messier, and K. E. Spear, Mater. Res. Bull. **23**, 531 (1988).

[17]A. T. Collins and S. C. Lawson, J. Phys. Condens. Matter **1**, 6929 (1989).

[18]K. Maier (private communication).

[19]C. D. Clark and C. B. Dickerson, Surf. Coatings Technol. **47**, 336 (1991).

[20]J. D. Wiley and J. A. Seman, Bell Syst. Tech. J. **50**, 355 (1970).

[21]P. R. Briddon and R. Jones, Physica B **185**, 179 (1993), and references therein.